Pumping effect measured by PIV method in multi-layer spike electrode EHD device for air cleaning

J. Podliński[1]*, A. Niewulis[1], A. Berendt[1], J. Mizeraczyk[1, 2]
[1] Centre for Plasma and Laser Engineering, The Szewalski Institute of Fluid Flow Machinery, Polish Academy of Sciences, Fiszera 14, 80-952 Gdańsk, Poland
[2] Department of Marine Electronics, Gdynia Maritime University, Morska 81-87, 81-225 Gdynia, Poland
* E-mail : janusz@imp.gda.pl

Abstract **— Dust particles can be harmful for human health when inhaled. Especially dangerous are submicron dust particles, which can contain traces of toxic elements and can easily penetrate into human respiratory system. Thus, new devices for air cleaning are needed. In this work the flow velocity field patterns measured by Particle Image Velocimetry (PIV) method in an electrohydrodynamic (EHD) device for air cleaning are presented. The EHD device had stressed electrodes with spike tips and grounded plates, and was similarly to those proposed by A. Katatani and A. Mizuno [J. Inst. Electrostat. Jpn., 34, 4 (2010)]. The parametric study of the flow velocity patterns was made for a different electrode arrangements.**

Index Terms **— electrohydrodynamics, electrostatic precipitators, fluid flow measurement, electrohydrodynamic pump, PIV, flow patterns.**

I. Introduction

When a strong electric field is generated between a sharp high voltage electrode and a grounded electrode, a corona discharge occurs resulting in an ionization of gas molecules. The ion flux along the electric field lines induces ionic wind, also known as the electrohydrodynamic (EHD) flow [1]-[6]. When the electrode arrangement results in an asymmetric electric field, an unidirectional gas flow can be produced (EHD gas pumping). However, in despite of that many electrode configurations were tested [7]-[10] the flow rate of the gas pumping in the investigated EHD pumps was unsatisfactory.

Recently, interesting results concerning EHD gas pumping were published by A. Katatani and A. Mizuno [11]. In their paper a self-ventilated multi-layer spike electrode electrostatic precipitator (ESP) was presented. The primary air flow (usually generated by conventional fans) was generated in this ESP by the EHD air flow induced by the corona discharge. A. Katatani and A. Mizuno performed many measurements in order to determine how the electrode geometry and position influence the induced flow velocity. They found that in general the gas flow velocity increased with rising applied voltage and with enlarging the distance ("G") and shift ("X") between high voltage and grounded electrodes (see Fig. 2). However, when the shift "X" was 30 mm, 50 mm and 90 mm a drop of the air flow velocity was observed for the high applied voltages. To understand the airflow generation in such a multi-layer ESP it is important to investigate the flow patterns produced close to the spike tips of the high voltage electrodes. Therefore, we decided to perform 2D particle image velocimetry (2D PIV) investigations in the EHD device (similar to that proposed by A. Katatani and A. Mizuno). The results of our investigations are presented below.

II. Experimental set-up

The experimental set-up for measurements of the flow patterns in the multi-layer spike electrode EHD device is presented in Fig. 1. It consisted of the EHD device, the high voltage supply and apparatus for flow measurements by the 2D PIV method.

The duct of the investigated multi-layer EHD device was made of a transparent acrylic box (600 mm long, 150 mm wide and 150 mm high). Inside this box in the middle of its length, a frame for sustaining spiked high voltage (HV) and grounded electrodes was placed. In the frame two sets of spiked high voltage and grounded electrodes made of 1 mm thick aluminium were mounted. The smooth, grounded electrode and spiked HV electrode were 124 mm wide and 150 mm long. The one of the edges of the HV electrode was ended with 20 spikes. These spikes were 10 mm long. The distance between neighbouring spike tips was 6 mm. The frame sustaining electrodes allowed mounting the HV and the grounded electrodes one above another, thus forming multi-layer electrode arrangement (Fig. 2). The distance G between the HV and the grounded electrodes could be changed. The electrodes could be also shifted in the x direction to change the electrode shift X between the edges of the neighbouring electrodes. For the distances G = 15 mm and G = 20 mm the flow patterns near the electrode spikes and the average velocity of the unidirectional flow in the EHD device duct were measured (using 2D PIV method) for the following electrode shift values: X = 8 mm, 15 mm and 50 mm.

When the distance G was 20 mm, an electrode set with 3 HV electrodes and 4 grounded electrodes was mounted in the EHD device. In the case of G = 15 mm, an electrode set of 4 HV electrodes and 5 grounded electrodes (like in Fig. 1) was formed.

The research presented in this paper was supported by the Ministry of Science and Higher Education grant PB 7475/B/T02/2011/40 and by the R. Szewalski Institute of Fluid Flow Machinery, Polish Academy of Sciences, Gdansk

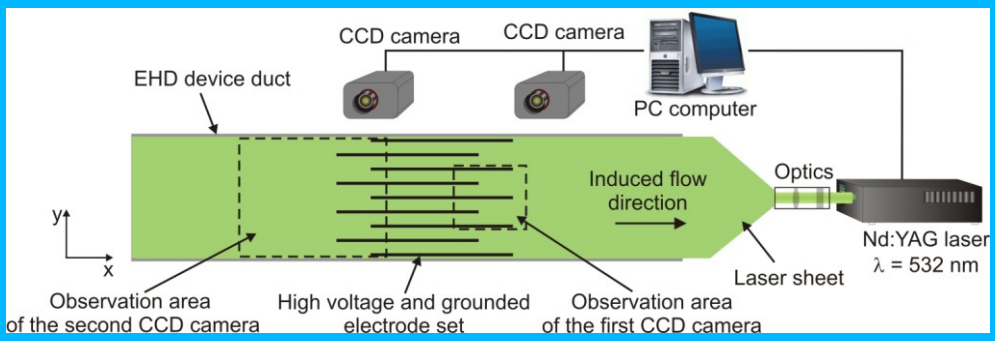

Fig. 1. Experimental set-up for the 2D PIV measurement of the airflow generated in the multi-layer spike electrode EHD device

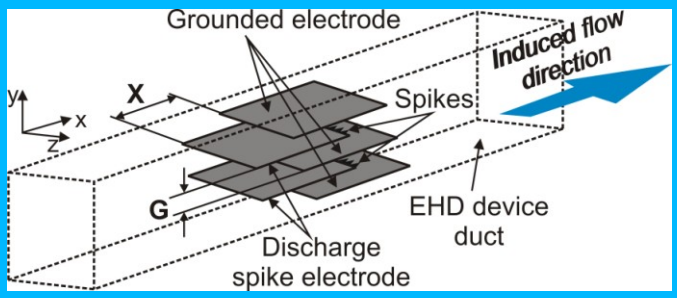

Fig. 2. Scheme of the EHD device for the air cleaning

Either the negative or positive DC high voltage (Spellman SL300 high voltage generator) was applied to the HV electrodes, the corona discharges were generated from each spike (Fig. 3). Each HV electrode was supplied through a resistor R = 3,33 MΩ. An average discharge current I and power supply output voltage U were measured by the meters installed on the high voltage supply output. Then, the discharge power P was calculated.

To the inlet of EHD device a PCV pipe (3 m long, 160 mm inner diameter) was connected. Before each PIV measurement the pipe and EHD device duct were filled up with cigarette smoke which was used as a seeding. Since, the EHD device was not equipped with any external fan, the unidirectional flow produced in the EHD device duct was induced only by the corona discharge.

The 2D PIV measurement system consisted of a double Nd:YAG laser system (λ = 532 nm), a cylindrical telescope, two CCD cameras (FlowSense M2 1600 pixels × 1186 pixels) and a PC computer. The PIV investigations were carried out in the plane fixed by a laser sheet shaped by the cylindrical telescope. The laser sheet was introduced in the centre of the EHD device duct, perpendicularly to the electrodes. The observation areas of the CCD cameras are marked in Fig. 1 with broken lines. The first CCD camera recorded PIV images of the EHD secondary flow around the spikes of the two central discharge electrodes. The observation area of the second CCD camera was placed at the EHD device inlet near the smooth edges of the electrodes. Basing on the PIV images recorded by the second camera the average velocity of the unidirectional flow in the EHD device duct was determined.

100 pairs of PIV instantaneous images of the flow were taken, and then an adaptive cross-correlation algorithm was applied to compute 100 instantaneous flow velocity fields. Next, the time-averaged flow velocity field was calculated from the 100 instantaneous flow velocity field. The interrogation window for the cross-correlation procedure was 32 pixels × 16 pixels (horizontal × vertical). The overlap of neighbouring interrogation windows was 25%.

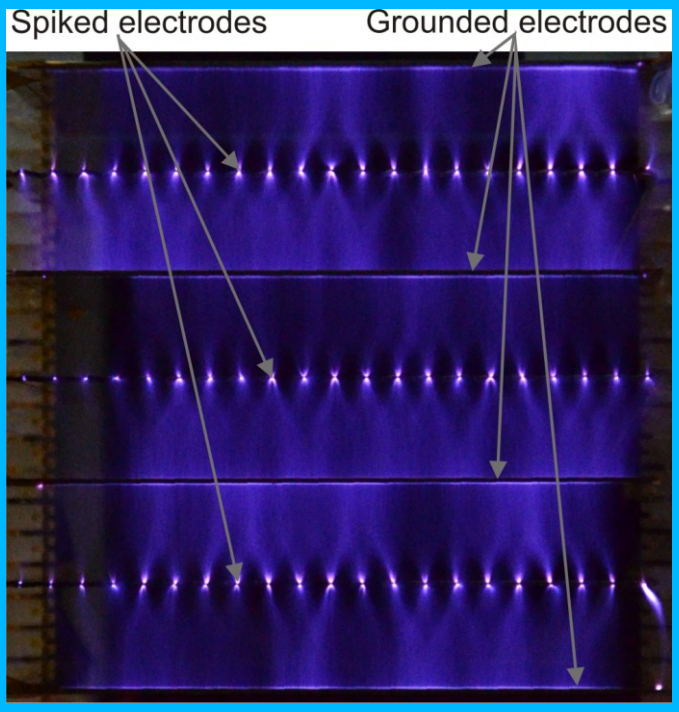

Fig. 3. Image of the corona discharges generated in the investigated EHD device (front view). The distance G was 20 mm and the shift X was 8 mm. DC high voltage of + 15 kV was applied. The camera exposure time was 1 s.

III. Results

The current-voltage characteristics of the multi-layer EHD device for air cleaning were measured for several investigated electrode arrangements. The current-voltage characteristics for G = 20 mm and G = 15 mm are presented in Figs. 4 and 5, respectively. As it is seen in these figures, in both cases the discharge current increased with increasing electrode shift X. For low applied voltages the discharge current was higher for the negative voltage polarity. However, when the applied

voltage increased the discharge current was higher for the positive polarity. It was pronounced when the distance G between HV electrodes and grounded electrodes was 20 mm. In particular, when the positive applied voltage exceeded 13 kV the discharge current was clearly higher than that measured for the negative voltage polarity. This may suggest that the positive corona discharge could be unstable, i.e. pre-breakdown streamers could occur.

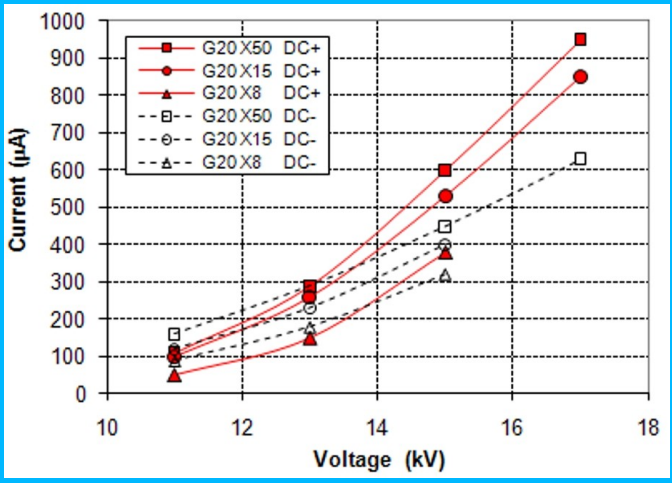

Fig. 4. Current-voltage characteristic of the EHD device, G = 20 mm

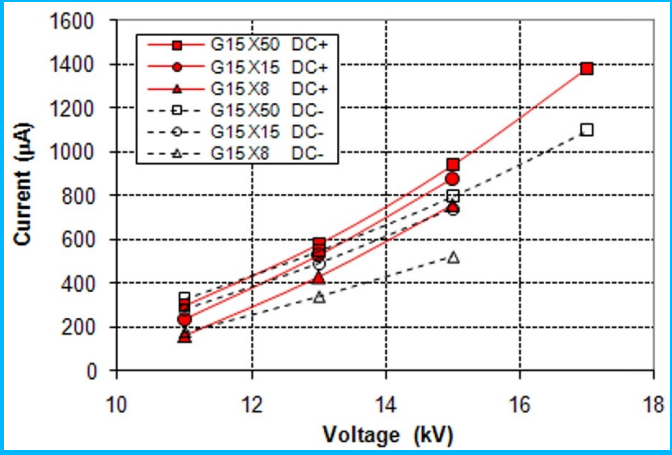

Fig. 5. Current-voltage characteristic of the EHD device, G = 15 mm

The 2D PIV measurements of the flow induced in the EHD device with the different electrode arrangements were performed. Basing on these measurements the flow patterns near the spike of HV electrodes and the average flow velocity induced in the EHD device duct were determined.

Examples of the obtained flow patterns (velocity vector maps and streamlines) measured near spikes of discharge electrodes are presented in Figs. 6-9. In Fig. 6 the velocity vector maps obtained for the distance G = 15 mm and shift X = 50 mm are shown. The applied high voltage U of positive polarity was +11 kV, +15 kV and +17 kV. As it is seen, behind the HV electrode spikes a jet-like flow was generated. On general, the flow velocity of this jet was higher for higher applied voltages. But, an increase in the applied voltage from +15 kV to +17 kV did not increase the jet velocity.

The jet-like flow induced vortices between the high voltage and the grounded electrodes. These vortices are easily visible when observing the streamlines of the produced flow. Figs. 7 and 8 show examples of the obtained streamlines in the EHD device for G = 15 mm and G = 20 mm (X = 8 mm, 15 mm and 50 mm). In these cases applied voltage was 15 kV (positive polarity for G = 15 mm, Fig. 7 and negative for G = 20 mm Fig. 8). As it is seen in these figures significant vortices between the spikes and the grounded electrodes were formed. For X = 8 mm, the vortices seems to fill almost the whole space between the HV and the grounded electrodes. For X = 15 mm the vortices are slightly smaller than for X = 8 mm, however, the smallest vortices were observed for X = 50 . The vortices diameter seems to be independent of voltage polarity. One may expect that strong vortex structures found in the EHD device are capable of hindering the induction of airflow in the EHD device. To check this supposition the average velocity of the unidirectional flow generated in the EHD device for various electrode arrangements was determined.

For this purpose, the flow patterns at the EHD device inlet were measured and then the velocity profile was determined at 40 mm before the rear edges of the HV electrodes. Basing on this velocity profile, the average velocity of the induced air flow was calculated. The dependence of the average flow velocity on applied voltage for G = 20 mm and G = 15 mm are shown in Figs. 9 and 10, respectively. As it can be seen, the average flow velocity increased with increasing applied voltage (with a tendency to saturation). However, the drop of the flow velocity reported by A. Katatani and A. Mizuno was not observed. The lowest average flow velocity was found for the X = 8 mm and the highest one for X = 50 mm (as we expected after the streamlines analysis). It seems that in the case of X = 8 mm the majority of applied electrical power was consumed for creating the vortex structures.

The obtained average velocities of the unidirectional air flow (Figs. 9 and 10) were slightly higher for negative voltage polarity. The difference in the average flow velocity for the negative and positive polarities was more pronounced for higher voltages (Figs. 9 and 10). Thus, the electrical efficiency of the unidirectional flow generation the in the EHD device was higher for the negative voltage.

We have also found that from the electrical efficiency point of view a slightly better electrode arrangement was for G = 20 mm (3 HV electrodes and 4 grounded electrodes) than for G = 15 mm (4 HV electrodes and 5 grounded electrodes) (Fig. 11).

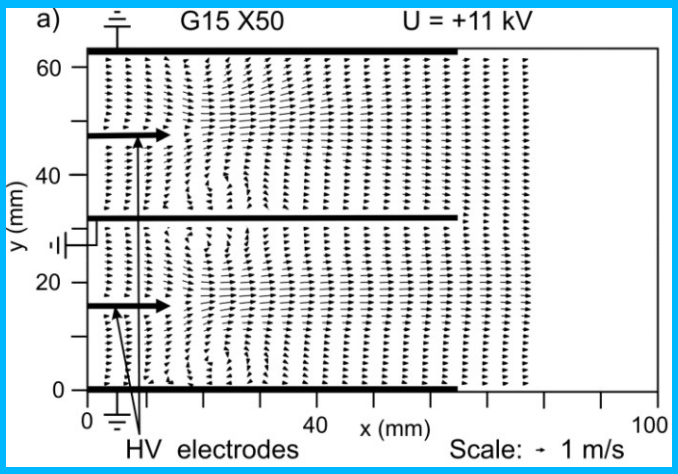

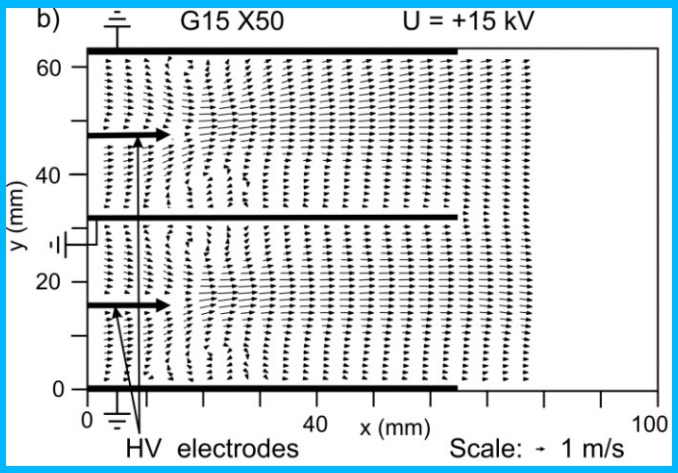

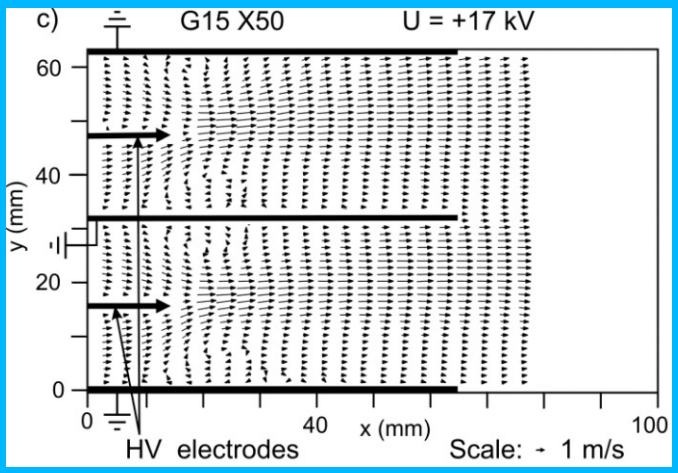

Fig. 6. Flow patterns (velocity vector map) measured by 2D PIV method in the area near the spike tips of the HV electrodes for the electrode arrangement with G = 15 mm and X = 50 mm. The applied positive high voltage was + 11 kV (a), + 15 kV (b), + 17 kV (c).

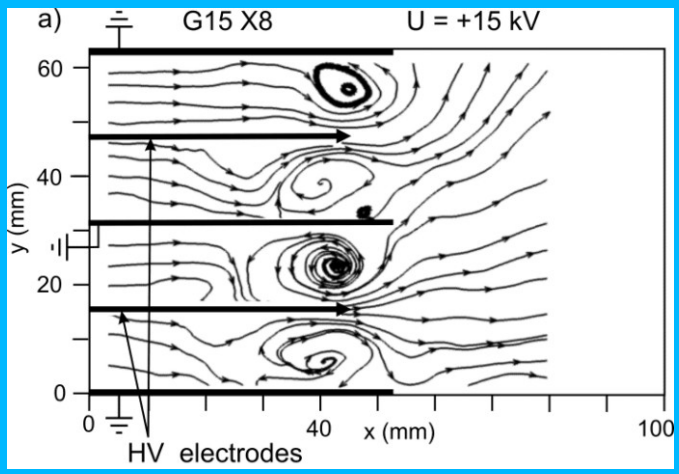

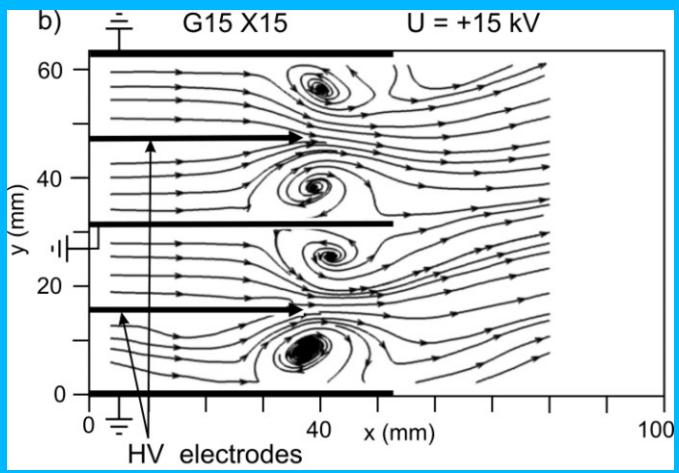

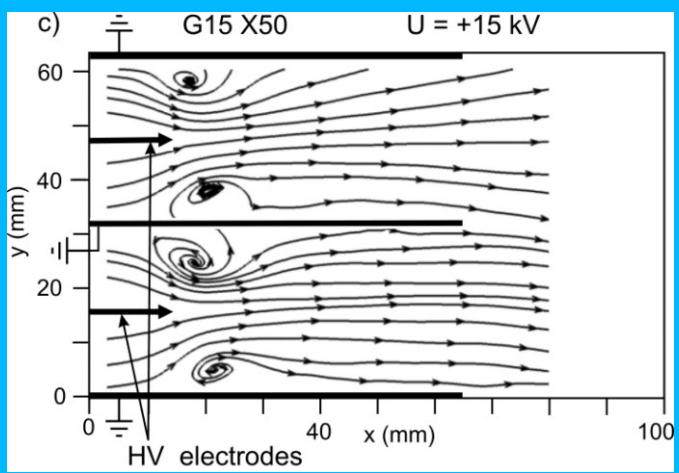

Fig. 7. Flow patterns (streamlines) measured by 2D PIV method in the area near the spike tips of the HV electrodes for the electrode arrangements with G = 15 mm, X = 8 mm (a), X = 15 mm (b), X = 50 mm (c). The applied positive high voltage was + 15 kV.

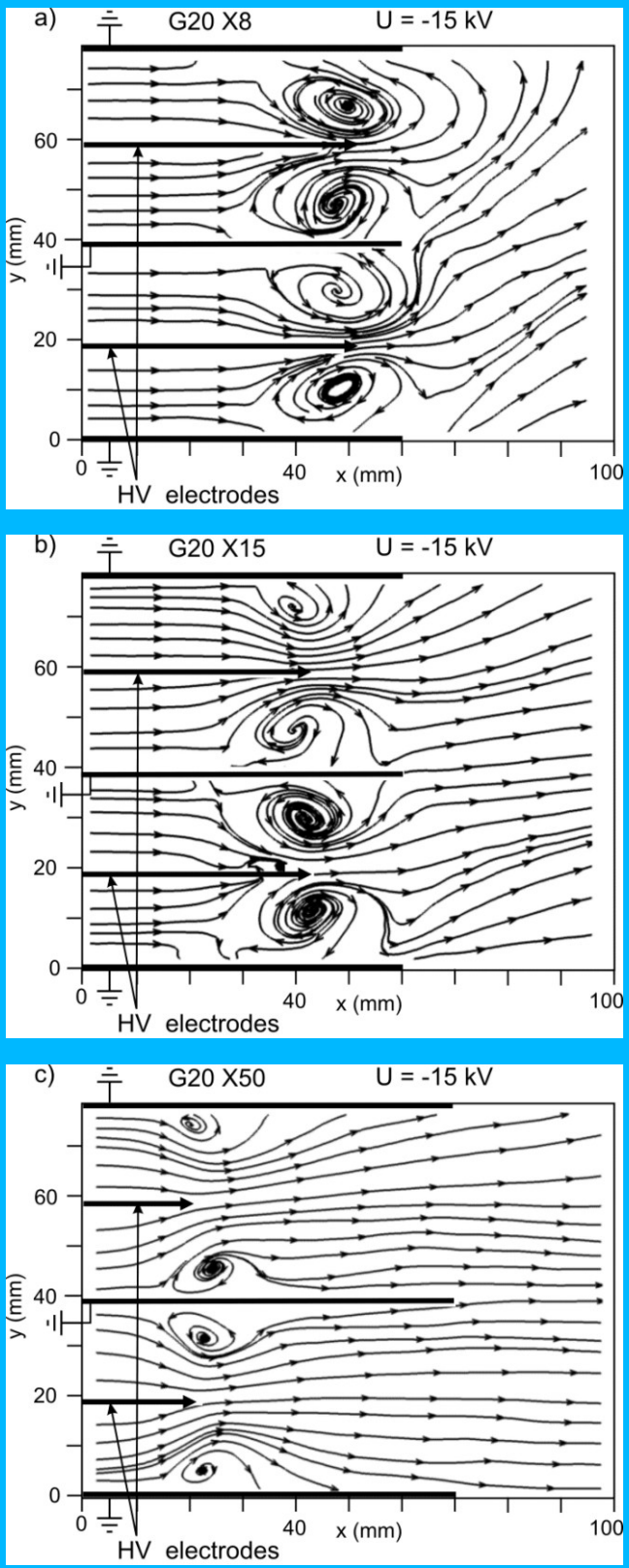

Fig. 8. Flow patterns (streamlines) measured by 2D PIV method in the area near the spike tips of the HV electrodes for the electrode arrangements with G = 20 mm, X = 8 mm (a), X = 15 mm (b), X = 50 mm (c). The applied negative high voltage was - 15 kV.

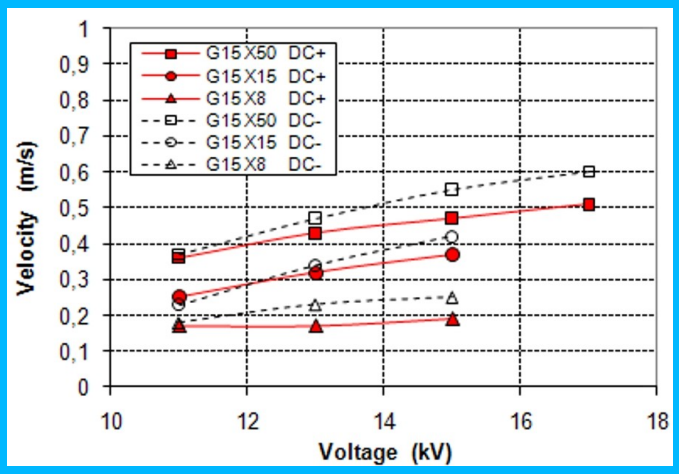

Fig. 9. The flow average velocity induced in the EHD device duct for G = 15 as a function of the applied voltage

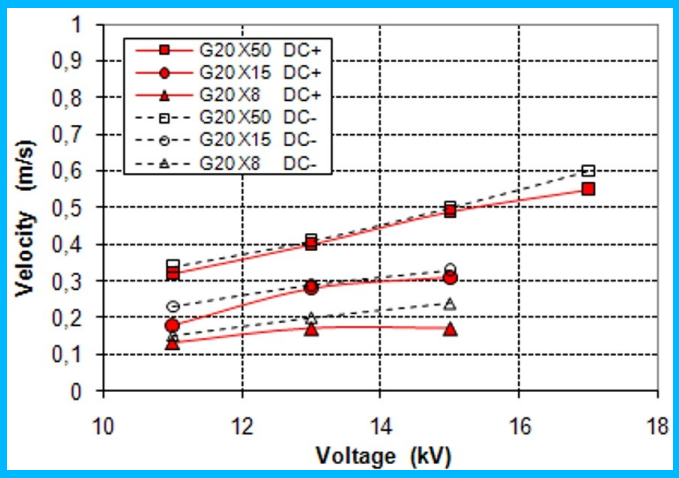

Fig. 10. The flow average velocity induced in the EHD device duct for G = 20 as a function of the applied voltage

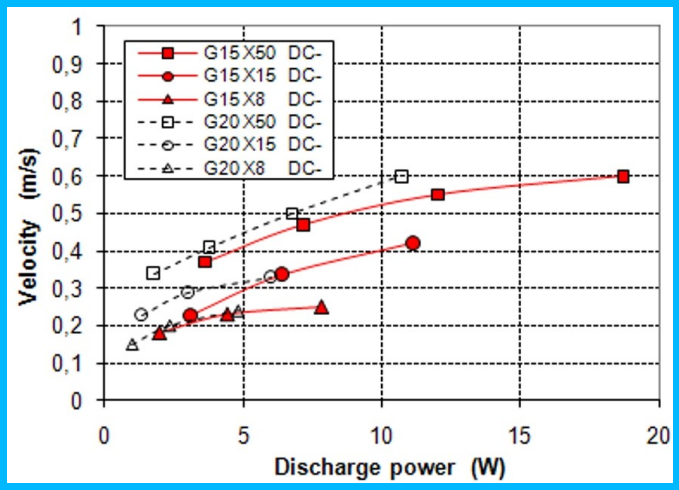

Fig. 11. The average velocity of air flow induced in the EHD device for G = 20 as a function of the discharge power

IV. SUMMARY

In this paper the pumping effect in the multi-layer spike electrode EHD device for gas cleaning was investigated using 2D PIV method. The results revealed generation of complex air flow patterns near the spike electrodes and a net unidirectional air flow in the EHD device.

The obtained flow patterns showed that jet-like air flow behind the tips of the spike electrodes was generated. The jet-like flow induced significant vortices between the spiked electrodes and the grounded electrodes. The diameters of the vortices depended on spiked electrode shift X in relation to the grounded electrode. When the electrode shift X was 8 mm vortices filled the whole space between the HV electrodes and the grounded electrodes. When, the electrode shift X was 50 mm only small vortices near the grounded electrodes were observed. We suggested that the reduction of vortices could be beneficial for inducing strong unidirectional flow in the EHD device duct. The results of the measurements of the average flow velocity at the EHD device inlet confirmed our suggestions.

The average velocity of the unidirectional flow increased with increasing applied voltage. For higher discharge powers the induced flow velocity increased slower that at lower ones with a tendency to saturation. However, the drop of the flow velocity reported by A. Katatani and A. Mizuno was not observed. The maximum average flow velocity of 0.6 m/s was obtained at a voltage of U = -17 kV for two electrode arrangements i.e. with G = 15 mm, X = 50 mm and with G = 20 mm, X = 50 mm.

The effect of the flow velocity saturation was stronger case for the positive polarity of the applied voltage. Presumably, this was caused by changes in the corona discharge character at higher voltages. The current-voltage characteristics seems to confirm this conclusion. When the applied voltage was higher than + 15 kV a rapid increase in the discharge current was observed. Such a discharge current increase could result by the formation of pre-breakdown streamers, which are probably disadvantageous for the gas flow generation.

Our research showed that investigated EHD device could be useful for a gas pumping. Further experiments will be performed to determine other factors that influence the flow generation in this EHD device. Also experiments concerning air cleaning in the EHD device will be carried out.

REFERENCES

[1] O. Stuetzer, *Ion drug pressure generation*, Journal of Applied Physics, vol. 30, no. 7, pp. 984-994, 1959.

[2] M. Robinson, "Movement of Air in the Electric Wind of the Corona Discharge", *Trans. Amer. Inst. Electr. Eng*., vol. 80, pp. 143–150, 1961.

[3] M. Robinson, "A history of the electric wind", Amer. J. Phys., vol. 30, pp. 366–372, 1962.

[4] S.H. Jeong and S.S Kim, "A Study on the Electrohydrodynamic Flow in a Rectangular Impactor with Positive Corona Discharge", *Aerosol Sci. Tech*., vol. 29, pp. 1-16, 1998.

[5] M. Rickard, D. Dunn-Rankin, F. Weinberg and F. Carleton, "Maximizing Ion-Driven Gas Flows", *J. Electrostat*., vol. 64, pp. 368–376, 2006.

[6] J.S. Chang, J. Ueno, H. Tsubone, G.D. Harvel, S. Minami and K. Urashima, "Electrohydrodynamically Induced Flow Direction in a Wire-Non-Parallel Plate Type Electrode Corona Discharge", *J. Phys. D; Appl. Phys*., vol. 40, pp. 5109-5111, 2007.

[7] L. Leger, E. Moreau, F. Artana and G. Touchard, "Influence of a DC corona discharge on the airflow along an inclined flat plate", *J. Electrost*., vol. 51–52, pp. 300–306, 2001.

[8] H. Yanada, S. Hakama, T. Miyashita and N. Zhang, "An investigation of an ion drag pump using a needle–mesh electrode configuration", *The Proc. Instn. Mech. Engrs., Part C: Journal of Mechanical Engineering Science*, vol. 216, no. 3 pp. 325-334, 2002.

[9] L. Zhao and K. Adamiak, "EHD flow in air produced by electric corona discharge in pin–plate configuration", *J. Electrostat*., vol. 63, pp. 337–350, 2005.

[10] H. Tsubone , J. Ueno, B. Komeili, S. Minami, G.D. Harvel, K. Urashima, C.Y. Ching and J.S. Chang, "Flow Characteristics of DC Wire-non-parallel Plate Electrohydrodynamic Gas Pump", *J. Electrostatics*, vol. 66, pp. 151-121, 2008.

[11] A. Katatani, A. Mizuno "Generation of Ionic Wind by Using Parallel Located Flat Plates", *J. Inst. Electrostat. Jpn*., vol. 34, no. 4, pp. 187-192, 2010.